

Supporting Information

Tailoring high-temperature stability and electrical conductivity of high entropy lanthanum manganite for solid oxide fuel cell cathodes

Yinchun Shi ^a, Na Ni ^{*abc}, Qi Ding ^d and Xiaofeng Zhao ^a

^a*School of Materials Science and Engineering, Shanghai Jiao Tong University, Shanghai 200240, China*

^b*Key Lab of Education Ministry for Power Machinery and Engineering, School of Mechanical Engineering, Shanghai Jiao Tong University, Shanghai 200240, China*

^c*Gas Turbine Research Institute, School of Mechanical Engineering, Shanghai Jiao Tong University, Shanghai 200240, China. E-mail: na.ni@sjtu.edu.cn*

^d*School of Mechanical Engineering, Shanghai Jiao Tong University, Shanghai 200240, China.*

Table S1 Average particle/ grain sizes and corresponding calcination/ sintering parameters of single-phase HEALMO and LSM82 powders and pellets. The calcination temperature was chosen as the minimum temperature at which a single-phase structure can be obtained after the precursor was calcinated for 2 h.

Composition	Powder		Pellet	
	Average particle size (nm)	Calcination parameter	Average grain size (μm)	Sintering parameter
HEALMO-1	520	1200°C for 2 h	3.85	1400°C for 10 h
HEALMO-2	360	1200 C for 2 h	4.28	1400°C for 10 h
HEALMO-3	220	1100 C for 2 h	1.75	1300°C for 10 h
LSM82	660	Unknown	10.74	1400°C for 5 h

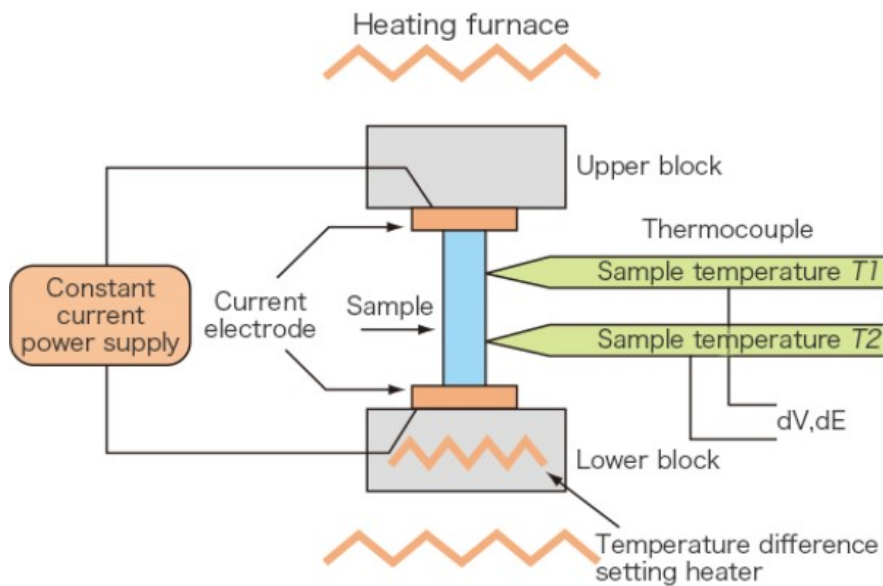


Fig. S1 Schematic diagram of electrical conductivity measurement via Seebeck coefficient/ electrical resistance measuring system, in which the current electrodes and thermocouples are made of platinum-rhodium alloy. The two parallel thermocouples are used to measure the voltage drop, and the corresponding parallel distance is 6 mm.

ADVANCE RIKO, Inc., <https://advance-riko.com/en/products/zem-3/>, (accessed September 2021).

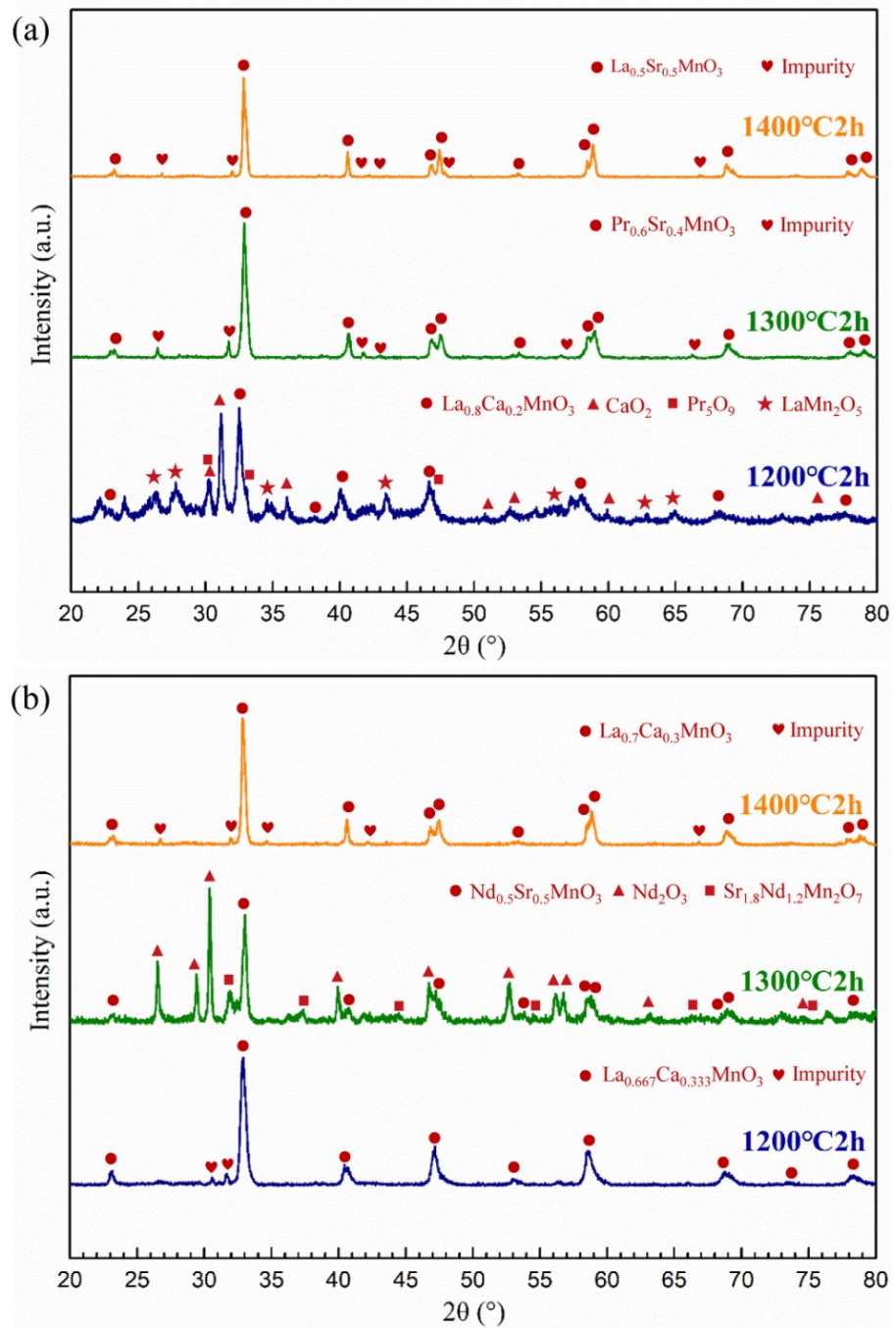


Fig. S2 XRD patterns of non-single-phase HEALMOs:

(a) HEALMO-4 and (b) HEALMO-5.

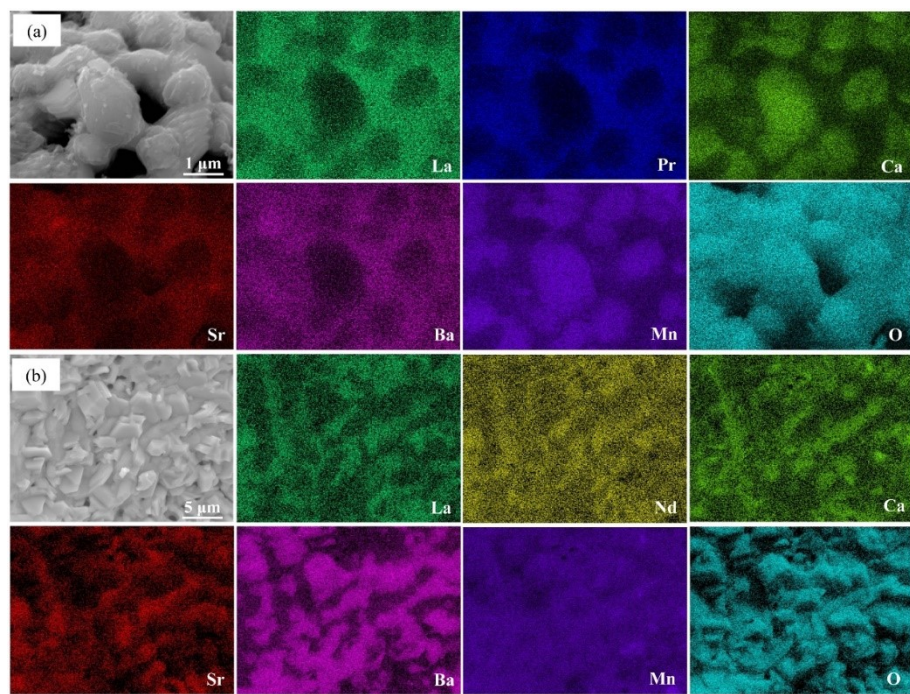


Fig. S3 Elemental distribution in non-single-phase HEALMOs:

(a) HEALMO-4 and (b) HEALMO-5.

Table S2 Average relative acidity of A site oxides in HEALMOs, and relative acidity of oxides related to HEALMOs.

Composition	Relative acidity	Composition	Relative acidity
HEALMO-1	1.252	Sm ₂ O ₃	1.274
HEALMO-2	0.995	Nd ₂ O ₃	1.139
HEALMO-3	1.069	CaO	1.099
HEALMO-4	0.987	Pr ₂ O ₃	1.064
HEALMO-5	1.002	SrO	0.978
Y ₂ O ₃	1.591	BaO	0.938
Gd ₂ O ₃	1.402	La ₂ O ₃	0.855

Table S3 Oxidation state, coordination number, ionic radii of A site cations, and prototype structure of the corresponding manganite associated with HEALMO-4 and HEALMO-5.

A site cation	Coordination number ^{1, 2}	Ionic radii (\AA) ^{1, 2}
La^{3+}	XII	1.36
Pr^{3+}	XII	1.32
Nd^{3+}	XII	1.27
Ca^{2+}	XII	1.34
Sr^{2+}	XII	1.44
Ba^{2+}	XII	1.61

Table S4 Crystal structure, space group, Goldschmidt's tolerance factor and cation size difference of conventional and high entropy perovskite oxides. To facilitate the comparison, Goldschmidt's tolerance factor (t) and cation size difference (δ) of reported materials from the literature were re-calculated according to Equation (3) and (4) in the manuscript using the ion radius values in Table S5.

Composition	Crystal structure	SG	Goldschmidt's	Cation size	Reference
			tolerance factor (t)	difference (δ)	
(La _{0.9} Ca _{0.1})MnO ₃	Orthorhombic	-	0.969	0.44%	3
(La _{0.6} Ca _{0.4})MnO ₃	Orthorhombic	<i>Pbnm</i>	0.967	0.72%	4
(La _{0.9} Sr _{0.1})MnO ₃	Orthorhombic	<i>Pbnm</i>	0.972	1.75%	5
(La _{0.9} Ba _{0.1})MnO ₃	Orthorhombic	<i>Pnma</i>	0.978	5.42%	6
(La _{0.8} Ca _{0.2})MnO ₃	Orthorhombic	<i>Pnma</i>	0.968	0.59%	7
(La _{0.7} Ca _{0.3})MnO ₃	Orthorhombic	<i>Pnma</i>	0.967	0.68%	
(La _{0.6} Sr _{0.4})MnO ₃	Orthorhombic	-	0.981	2.82%	
(La _{0.5} Sr _{0.5})MnO ₃	Orthorhombic	-	0.984	2.86%	
(Pr _{0.9} Sr _{0.1})MnO ₃	Orthorhombic	-	0.960	2.70%	
(Pr _{0.8} Sr _{0.2})MnO ₃	Orthorhombic	-	0.964	3.57%	
(Pr _{0.7} Sr _{0.3})MnO ₃	Orthorhombic	-	0.968	4.06%	
(Pr _{0.6} Sr _{0.4})MnO ₃	Orthorhombic	-	0.973	4.30%	
(Pr _{0.5} Sr _{0.5})MnO ₃	Orthorhombic	-	0.977	4.35%	
(Nd _{0.9} Sr _{0.1})MnO ₃	Orthorhombic	-	0.944	3.96%	
(Nd _{0.8} Sr _{0.2})MnO ₃	Orthorhombic	-	0.950	5.21%	
(Nd _{0.7} Sr _{0.3})MnO ₃	Orthorhombic	-	0.956	5.90%	
(Nd _{0.6} Sr _{0.4})MnO ₃	Orthorhombic	-	0.962	6.22%	8
(Nd _{0.5} Sr _{0.5})MnO ₃	Orthorhombic	-	0.968	6.27%	
(Sm _{0.9} Sr _{0.1})MnO ₃	Orthorhombic	-	0.935	4.76%	
(Sm _{0.8} Sr _{0.2})MnO ₃	Orthorhombic	-	0.942	6.25%	
(Sm _{0.7} Sr _{0.3})MnO ₃	Orthorhombic	-	0.948	7.05%	
(Sm _{0.6} Sr _{0.4})MnO ₃	Orthorhombic	-	0.955	7.42%	
(Sm _{0.5} Sr _{0.5})MnO ₃	Orthorhombic	-	0.963	7.46%	
(Gd _{0.9} Sr _{0.1})MnO ₃	Orthorhombic	-	0.944	3.96%	
(Gd _{0.8} Sr _{0.2})MnO ₃	Orthorhombic	-	0.950	5.21%	
(Gd _{0.7} Sr _{0.3})MnO ₃	Orthorhombic	-	0.956	5.90%	
(Gd _{0.6} Sr _{0.4})MnO ₃	Orthorhombic	-	0.962	6.22%	
(Gd _{0.5} Sr _{0.5})MnO ₃	Orthorhombic	-	0.968	6.27%	
(Gd _{0.5} Sr _{0.5})CoO ₃	Orthorhombic	<i>Pnma</i>	0.985	6.27%	
(Nd _{0.5} Ba _{0.5})CoO ₃	Orthorhombic	<i>Pmmm</i>	1.016	11.81%	
(Gd _{0.5} Ba _{0.5})CoO ₃	Orthorhombic	<i>Pmmm</i>	1.016	11.81%	
(La _{0.5} Sr _{0.5})CoO ₃	Rhombohedral	$\bar{R}\bar{3}c$	1.001	2.86%	9
(Pr _{0.5} Sr _{0.5})CoO ₃	Rhombohedral	$\bar{R}\bar{3}c$	0.994	4.35%	
(Nd _{0.5} Sr _{0.5})CoO ₃	Rhombohedral	$\bar{R}\bar{3}c$	0.985	6.27%	
(La _{0.5} Ba _{0.5})CoO ₃	Rhombohedral	$\bar{R}\bar{3}c$	1.032	8.42%	
(La _{0.8} Ba _{0.2})MnO ₃	Rhombohedral	$\bar{R}\bar{3}c$	0.987	7.09%	

$(La_{0.7}Ba_{0.3})MnO_3$	Rhombohedral	$R\bar{3}c$	0.996	7.98%	
$(La_{0.7}Sr_{0.3})MnO_3$	Rhombohedral	$R\bar{3}c$	0.978	2.65%	7
$(Sr_{0.9}Ho_{0.1})CoO_3$	Cubic	$Pm\bar{3}m$	1.008	4.44%	10
$(Sm_{0.4}Sr_{0.6})CoO_3$	Cubic	-	0.987	7.20%	
$(Sm_{0.3}Sr_{0.7})CoO_3$	Cubic	-	0.994	6.64%	
$(Sm_{0.2}Sr_{0.8})CoO_3$	Cubic	-	1.001	5.71%	
$(Sm_{0.1}Sr_{0.9})CoO_3$	Cubic	-	1.008	4.23%	11
$(Dy_{0.3}Sr_{0.7})CoO_3$	Cubic	-	0.994	6.64%	
$(Dy_{0.2}Sr_{0.8})CoO_3$	Cubic	-	1.001	5.71%	
$(Dy_{0.1}Sr_{0.9})CoO_3$	Cubic	-	1.008	4.23%	
$(La_{0.2}Nd_{0.2}Sm_{0.2}Y_{0.2}Gd_{0.2})CoO_3$	Orthorhombic	$Pbnm$	0.945	7.49%	
$(La_{0.2}Nd_{0.2}Sm_{0.2}Y_{0.2}Gd_{0.2})CrO_3$	Orthorhombic	$Pbnm$	0.927	7.49%	
$(La_{0.2}Nd_{0.2}Sm_{0.2}Y_{0.2}Gd_{0.2})FeO_3$	Orthorhombic	$Pbnm$	0.936	7.49%	
$La(Co_{0.2}Cr_{0.2}Fe_{0.2}Mn_{0.2}Ni_{0.2})O_3$	Orthorhombic	$Pbnm$	0.978	2.63%	12
$Gd(Co_{0.2}Cr_{0.2}Fe_{0.2}Mn_{0.2}Ni_{0.2})O_3$	Orthorhombic	$Pbnm$	0.946	2.63%	
$Sm(Co_{0.2}Cr_{0.2}Fe_{0.2}Mn_{0.2}Ni_{0.2})O_3$	Orthorhombic	$Pbnm$	0.935	2.63%	
$Nd(Co_{0.2}Cr_{0.2}Fe_{0.2}Mn_{0.2}Ni_{0.2})O_3$	Orthorhombic	$Pbnm$	0.946	2.63%	
$Y(Co_{0.2}Cr_{0.2}Fe_{0.2}Mn_{0.2}Ni_{0.2})O_3$	Orthorhombic	$Pbnm$	0.880	2.63%	
$(La_{0.2}Pr_{0.2}Nd_{0.2}Sm_{0.2}Sr_{0.2})MnO_{3-\delta}$	Orthorhombic	$Pnma$	0.958	5.30%	13
$La(Mn_{0.2}Fe_{0.2}Co_{0.2}Ni_{0.2}Cu_{0.2})O_{3-\delta}$	Hexagonal	$R\bar{3}cH$	0.966	9.15%	14
$Ba(Zr_{0.2}Ti_{0.2}Sn_{0.2}Hf_{0.2}Y_{0.2})O_3$	Cubic	$Pm\bar{3}m$	1.001	13.30%	
$Ba(Zr_{0.2}Ti_{0.2}Sn_{0.2}Hf_{0.2}Nb_{0.2})O_3$	Cubic	$Pm\bar{3}m$	1.026	6.50%	15
$Ba(Zr_{0.2}Ti_{0.2}Sn_{0.2}Hf_{0.2}Ta_{0.2})O_3$	Cubic	$Pm\bar{3}m$	1.026	6.50%	
$Sr(Zr_{0.2}Sn_{0.2}Ti_{0.2}Hf_{0.2}Mn_{0.2})O_3$	Cubic	$Pm\bar{3}m$	0.972	7.34%	
$Sr(Zr_{0.2}Sn_{0.2}Ti_{0.2}Hf_{0.2}Nb_{0.2})O_3$	Cubic	$Pm\bar{3}m$	0.968	6.50%	
$Ba(Zr_{0.2}Sn_{0.2}Ti_{0.2}Hf_{0.2}Ce_{0.2})O_3$	Cubic	$Pm\bar{3}m$	1.004	11.92%	16
$Ba(Zr_{0.2}Sn_{0.2}Ti_{0.2}Hf_{0.2}Y_{0.2})O_{3-x}$	Cubic	$Pm\bar{3}m$	1.001	13.30%	
$Ba(Zr_{0.2}Sn_{0.2}Ti_{0.2}Hf_{0.2}Nb_{0.2})O_3$	Cubic	$Pm\bar{3}m$	1.026	6.50%	

Table S5 Ion radius values used to re-calculate Goldschmidt's tolerance factor (t) and cation size difference (δ)

of reported materials are listed in Table S2. The “LS” in Table means “low spin”, and “HS” means “high spin”.

Cation	Coordination number ^{1, 2}	Ionic radii (\AA) ^{1, 2}
La ³⁺	XII	1.36
Nd ³⁺	XII	1.27
Sm ³⁺	XII	1.24
Gd ³⁺	XII	1.27
Pr ³⁺	XII	1.32
Ca ²⁺	XII	1.34
Sr ²⁺	XII	1.44
Ba ²⁺	XII	1.61
Ho ³⁺	XII	1.23
Dy ³⁺	XII	1.24
Y ³⁺	IX	1.075
Y ³⁺	VI	0.90
Ti ⁴⁺	VI	0.605
Zr ⁴⁺	VI	0.72
Sn ⁴⁺	VI	0.69
Hf ⁴⁺	VI	0.71
Nb ⁵⁺	VI	0.64
Ta ⁵⁺	VI	0.64
Ce ⁴⁺	VI	0.87
Cr ³⁺	VI	0.615
Fe ³⁺	VI	0.55 ^{LS} , 0.645 ^{HS}
Co ³⁺	VI	0.545 ^{LS} , 0.61 ^{HS}
Ni ³⁺	VI	0.56 ^{LS} , 0.60 ^{HS}
Mn ³⁺	VI	0.58 ^{LS} , 0.645 ^{HS}
O ²⁻	VI	1.40

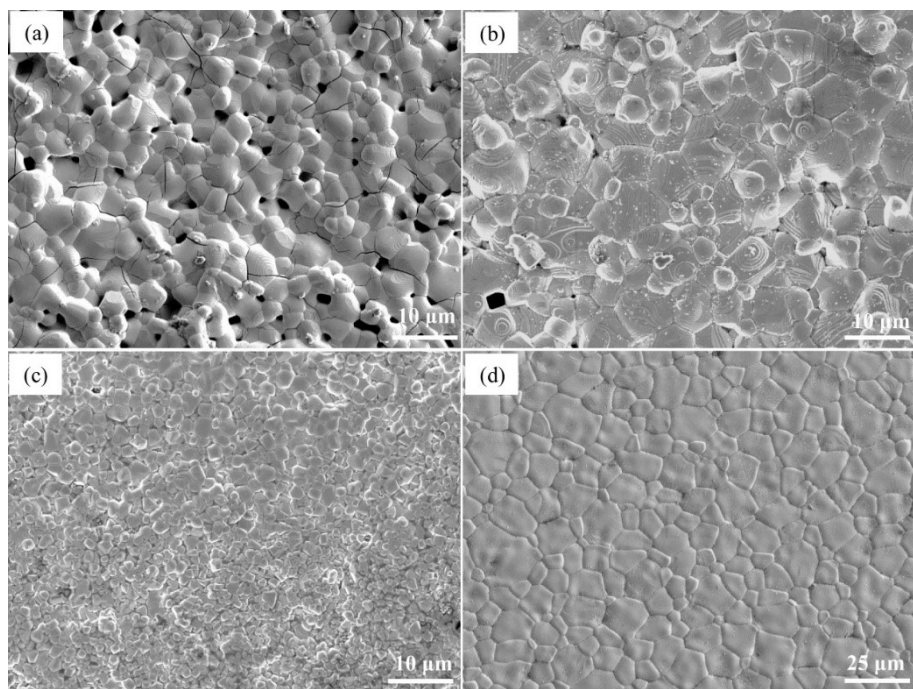


Fig. S4 Morphology of sintered pellets of HEALMOs and LSM82:

(a) HEALMO-1, (b) HEALMO-2, (c)HEALMO-3 and (d) LSM82.

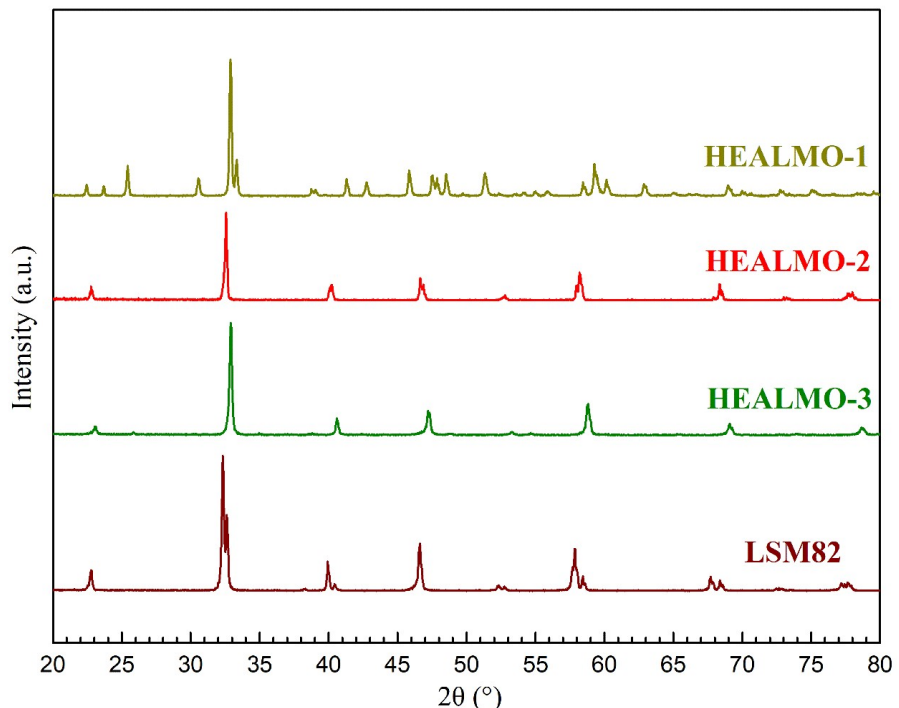


Fig. S5 XRD patterns of HEALMOs and LSM82 rectangle bars after electrical conductivity and Seebeck coefficient measurement.

References

- 1 R. D. Shannon, *Acta Crystallogr., Sect. A*, 1976, DOI: 10.1107/S0567739476001551.
- 2 Y.-Q. Jia, *J. Solid State Chem.*, 1991, **95**, 184-187.
- 3 T. Hashimoto, N. Ishizawa, N. Mizutani and M. Kato, *J. Mater. Sci.*, 1988, **23**, 1102–1105.
- 4 R.-S. Liu, C.-H. Shen and S.-F. Hu, *Int. J. Inorg. Mater.*, 2001, **3**, 1063–1072.
- 5 S. Xu, Y. Moritomo, K. Ohoyama and A. Nakamura, *J. Phys. Soc. Jpn.*, 2003, **72**, 709–712.
- 6 V. A. Cherepanov, E. A. Filonova, V. I. Voronin and I. F. Berger, *J. Solid State Chem.*, 2000, **153**, 205–211.
- 7 S. J. Hibble, S. P. Cooper, A. C. Hannon, I. D. Fawcett and M. Greenblatt, *J. Phys. Condens. Matter*, 1999, **11**, 9221–9238.
- 8 Y. Sakaki, Y. Takeda, A. Kato, N. Imanishi, O. Yamamoto, M. Hattori, M. Iio and Y. Esaki, *Solid State Ionics*, 1999, **118**, 187–194.
- 9 P. V. Vanitha, A. Arulraj, P. N. Santhosh and C. N. R. Rao, *Chem. Mater.*, 2000, **12**, 1666–1670.
- 10 T. Liu, L. Li and J.-K. Yu, *Ionics*, 2015, **22**, 853–858.
- 11 H.-Y. Tu, Y. Takeda, N. Imanishi and O. Yamamoto, *Solid State Ionics*, 1997, **100**, 283–288.
- 12 A. Sarkar, R. Djenadic, D. Wang, C. Hein, R. Kautenburger, O. Clemens and H. Hahn, *J. Eur. Ceram. Soc.*, 2018, **38**, 2318–2327.
- 13 Y. Yang, H. Bao, H. Ni, X. Ou, S. Wang, B. Lin, P. Feng and Y. Ling, *J. Power Sources*, 2021, DOI: 10.1016/j.jpowsour.2020.228959.
- 14 X. Han, Y. Yang, Y. Fan, H. Ni, Y. Guo, Y. Chen, X. Ou and Y. Ling, *Ceram. Int.*, 2021, DOI: 10.1016/j.ceramint.2021.03.052.
- 15 S. Zhou, Y. Pu, Q. Zhang, R. Shi, X. Guo, W. Wang, J. Ji, T. Wei and T. Ouyang, *Ceram. Int.*, 2020, **46**, 7430–7437.
- 16 S. Jiang, T. Hu, J. Gild, N. Zhou, J. Nie, M. Qin, T. Harrington, K. Vecchio and J. Luo, *Scr. Mater.*, 2018, **142**, 116–120.